

Development of Efficient Vertical Axis Wind Turbines

Comparative Experimental Study of a Small VAWT in Fixed Pitch and Variable Pitch Configurations

2022/04/06

Grzegorz Kawiecki, PhD



SUMMARY

This document presents the results of a comparative study of two basic Vertical Axis Wind Turbine configurations: a classical one with fixed blade pitch and a novel configuration with passive blade pitch control using a linkage mechanism with a center of rotation eccentric with respect to turbine's vertical axis.

Experimental results have shown that the variable pitch configuration is much more efficient in energy extraction from low and moderate velocity winds. In addition, this advantage has been much more pronounced for low load resistance values, typical for applications of growing importance, such as charging car batteries or battery banks for renewable energy storage used in urban or residential environments. To the best of my knowledge, this is the only study to compare experimentally both configurations, using the same basic test specimen.

This work has been inspired by research done by Benedict and Chopra, 2016, and Erickson et al, 2011. It has been carried out in my garage during the pandemic lockdown.

Introduction

I have designed, manufactured, and tested a Vertical Axis Wind Turbine of 400 mm diameter and 400 mm blade length. Blade airfoil is NACA 0021, with a chord length of 100 mm. This machine has been designed to work in two different configurations:

- conventional, with fixed blade pitch that, however, may be adjusted between -20° and $+20^\circ$, with a 10° step (when the rotor is not in motion, see Fig. 1), and
- novel, with passive blade pitch control, achieved through a system of control links, see Fig. 2.

In this report, the former will be called “fixed pitch configuration,” and the latter “variable pitch configuration.” Configuration change was achieved by interchanging specially designed blade-arm unions, see Fig. 1.

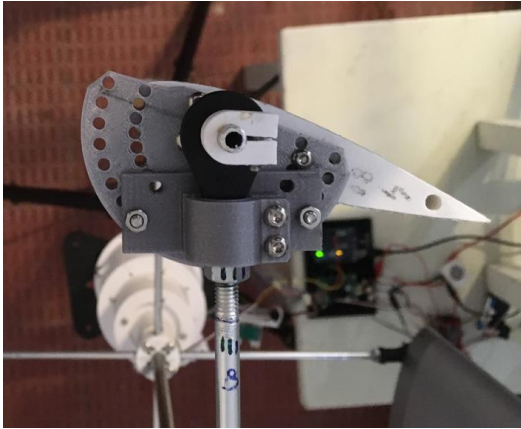


Fig. 1 The system for changing blade pitch magnitude, when the rotor is at rest.

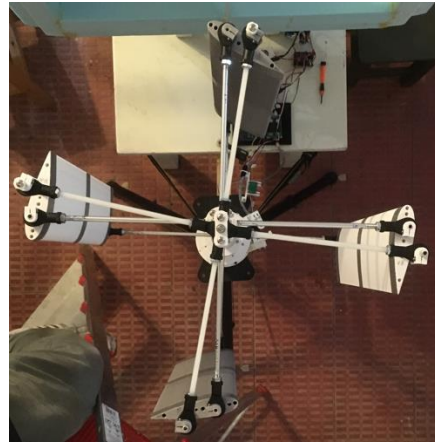


Fig. 2 Control links system designed to set blade pitch to a maximum at the windward side of the rotor, to a minimum at leeward side, and close to zero at each side of the rotor.

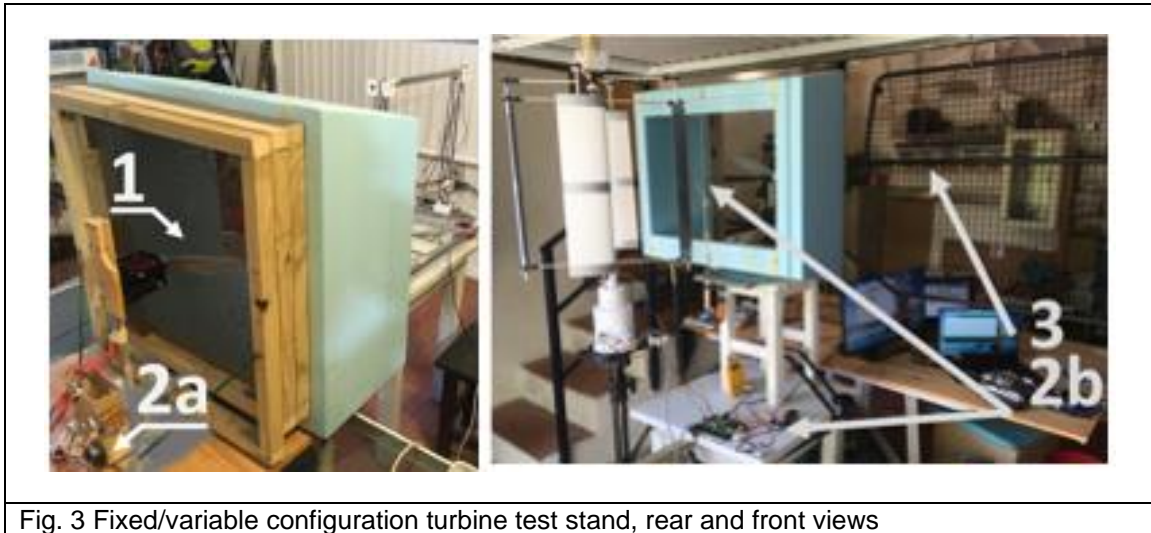
I have compared power output for fixed pitch and variable pitch turbine configurations, with the following results:

- The power output of the variable pitch turbine was far superior for low and moderate wind velocity for all tested load resistor values. Variable pitch turbine configuration performed better for strong winds and the *lowest* electrical resistance value tested. Please note that low electrical resistance values are typical for loads such as electric car batteries (~ 0.3 Ohm see, e.g., Miao, 2019) or residential banks of batteries.
- The cut-in wind velocity is much lower for the variable pitch configuration.
- Nearly half of the “parasitic power” needed to rotate the turbine is contributed by the aerodynamic resistance generated by moving structure elements.
- Measurements of electrical power for both configurations proved to be less accurate than mechanical power measurements on turbine’s shaft. The reason was probably the dependency of generator efficiency on its angular velocity and, possibly, the fact that the current sensor had a resolution of 0.05 A, what was good enough only for low load resistance values and high turbine RPM/output voltage generated.

Approach

Experimental configuration comparison has been carried-out using a system consisting of:

- A brushless 2.2 kW motor (by Hacker), with a 503x230 propeller,
- A custom-fabricated contraction nozzle with a 500 mm x 500 mm entrance cross-section and 400 mm x 500 mm exit cross section, equipped with a twin turbulence reduction mesh for some tests, see Fig. 3/1.
- A data turbine performance data acquisition and processing system consisting of:
 - two Data Acquisition modules from EagleTree, with 16 channels and sampling frequency up to 40 Hz,
 - Arduino Uno for acquisition of data produced by a load cell with HX711 controller, used to measure the torque produced at the shaft of the turbine
 - Pitot tube to measure the benchmark airflow velocity at the axis of symmetry of the flow streamtube that activates the turbine.
- A flow distribution scanning system consisting of:
 - a mobile frame run by two step motors controlled by open source GRBL software and enabling the Pitot tube to travel along a programmed path in 2d, to sample the airflow velocity at selected points. The same frame was used to fabricate the contracting nozzle, after replacing the Pitot tube with a hot wire styrofoam cutter, see Fig. 3/2a, 2b, A5,
 - an EagleTree DA module.
- A safety mesh, see Fig. 3/3.



A stepper motor with nominal velocity of 600 RPM and voltage of 24 V has been used as a two-phase generator (see Anon, 2020). The generator output was transmitted through a custom-designed and fabricated two-phase, AC/DC rectifier, to a variable resistor that simulated the electrical load. See the Appendix for the details of system fabrication and calibration process.

That system has been used to measure the performance of the turbine in both configurations, through the acquisition of selected input and output parameters. Measured input parameters were:

- The angular velocity of the propeller – the principal input parameter - controlled manually using an R/C radio transmitter, acquired, displayed real-time and stored using an EagleTree DA module,

- current and voltage measured at the terminals of a battery bank supplying the Hacker motor.
- airflow velocity measured at the longitudinal axis of the propeller-generated streamtube, at 400 mm from the propeller plane,
- load variable resistor.

The output parameters are:

- VAWT rotational velocity,
- reaction force measured at a mechanical stop preventing the generator from rotation, proportional to the moment at VAWT's shaft and the mechanical power generated. The latter being a product of the reaction force, moment arm, turbine angular velocity and the transmission ratio, if any.
- voltage and current measured at output terminals of the two-phase AC/DC rectifier. As indicated before, current measurements were not reliable for high load resistance values and low VAWT RPM/output voltage.

Each of the two configurations has been tested for the same set of input variables combinations of load resistance, blade pitch and wind velocity.

Output variables have been obtained for the following input parameters:

- load variable resistance values of 10, 25, 50 y 100 Ohm,
- propeller rotational velocities of 1500, 1900, and 2300 RPM that generated flow velocities at the Pitot tube location of 12, 17 and 22 km/h, respectively and VAWT rotational velocities reaching 400 RPM. Higher propeller and turbine rotational velocities have not been tested due to concerns about VAWT structural integrity.
- Pitch values of 0°, 10° y 20° (positive toe-out) for the fixed pitch configuration and -11°, -25° y -35° (measured at the leeward side) for the variable pitch configuration.

Tested input parameter combinations are laid out in Tables 1 and 2:

Table 1 Input parameters: fixed pitch configuration												
Pitch (°)	0				10				20			
R (Ohm)	10	25	50	100	10	25	50	100	10	25	50	100
Wind (km/h)	12	12	12	12	12	12	12	12	12	12	12	12
	17	17	17	17	17	17	17	17	17	17	17	17
	22	22	22	22	22	22	22	22	22	22	22	22

Table 2 Input parameters: variable pitch configuration												
Pitch (°)	-11				-25				-35			
R (Ohm)	10	25	50	100	10	25	50	100	10	25	50	100
Wind (km/h)	12	12	12	12	12	12	12	12	12	12	12	12
	17	17	17	17	17	17	17	17	17	17	17	17
	22	22	22	22	22	22	22	22	22	22	22	22

Each test run for the variable pitch configuration includes three 60 seconds–long intervals with constant propeller angular velocity, of 1500, 1900 and 2300 RPM, what corresponds approximately to 12, 17 and 22 km/h, respectively. Runs done for the fixed pitch configuration had the 22 km/h interval extended to 120 s, to give the turbine a chance to speed up to a measurable velocity. The general observation was that the fixed pitch configuration had a far higher cut-in velocity and even then would accelerate very slowly, in a sharp difference from the variable pitch configuration.

Results

Best performance, among the selected input parameters, has been obtained for:

- the variable pitch configuration with pitch of -11° (measured at the leeward side), and
- the fixed pitch configuration with pitch of 10° .

See Figs. 4-7:

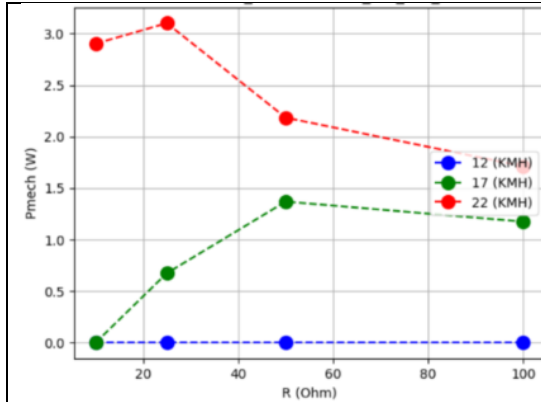


Fig. 4 **Fixed pitch configuration:** mechanical power vs load resistor value vs wind velocity, for 10° pitch.

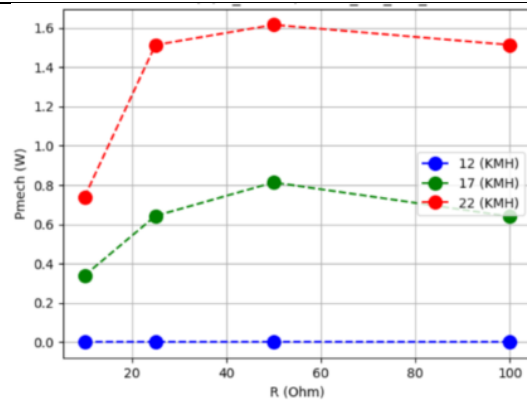


Fig. 5 **Fixed pitch configuration:** mechanical power vs load resistor value vs wind velocity, for 20° pitch.

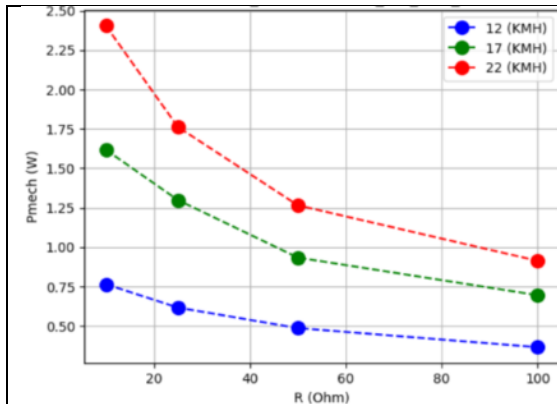


Fig. 6 **Variable pitch configuration:** mechanical power vs load resistor value vs wind velocity, for -11° pitch.

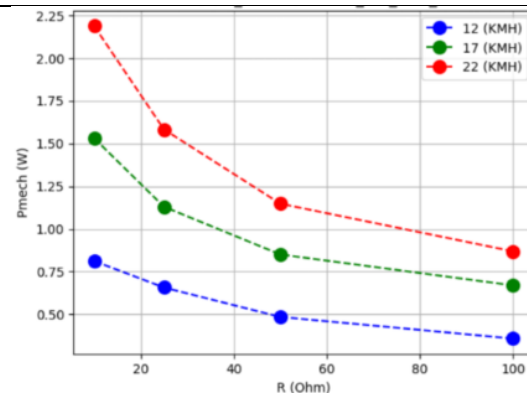


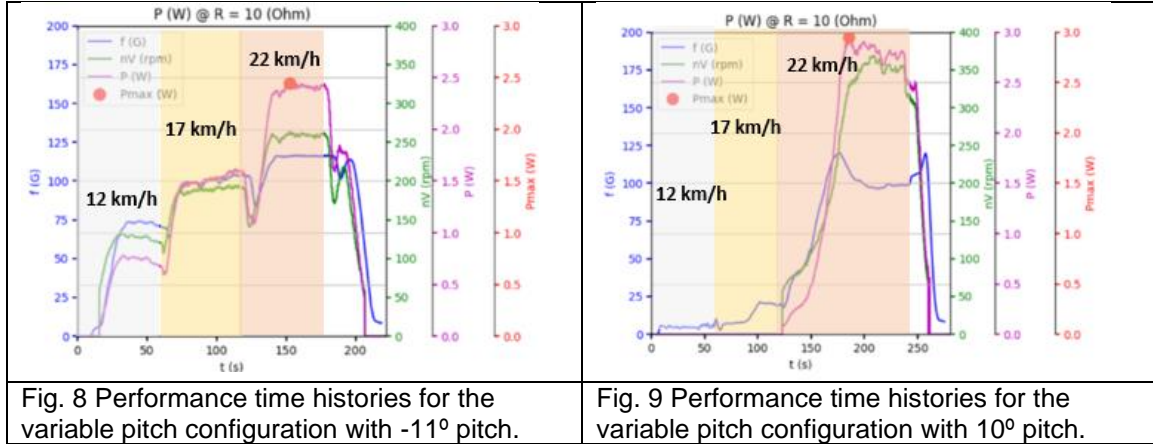
Fig. 7 **Variable pitch configuration:** mechanical power vs load resistor value vs wind velocity, for -25° pitch.

The lowest tested load resistance of 10 Ohm appears to be the closest to the expected resistance for one of the most likely applications – battery bank charging.

For that electrical resistance the fixed pitch configuration generates the most significant amount of mechanical power, for the highest tested wind velocity of 22 km/h. However, considering the growing tendency of power vs load resistance performance for variable pitch configuration and the decreasing tendency for fixed pitch configuration (confirmed for other pitch values, not shown here) it is quite possible that the variable configuration would be better than the fixed configuration also for wind velocity of 22 km/h - for load resistance somewhat lower than 10 Ohm.

Please note that the fixed pitch configuration had been tested at somewhat more favorable conditions. In order to achieve meaningful results. The reason for permitting this inequality was an extremely slow acceleration of the fixed pitch rotor, which needed much more time than the variable pitch configuration to achieve top performance for a given wind velocity. Please see

Figs. 8 and 9 that illustrate the temporal behavior of both configurations for the load resistance of 10 Ohm, where purple plots show produced power vs time, green plots indicate VAWT rotor RPM vs time and blue plots the reaction force, proportional to mechanical power produced at VAWT shaft. Steps visible in in time histories of variable pitch configuration output correspond to increments in wind velocity (12 km/h, 17 km/h, 22 km/h). We can see that the variable pitch configuration starts up and accelerates very rapidly to its top performance for a given wind velocity, while the fixed pitch configuration needs much more time, i.e., would need sustained moderate or strong winds to start up. That observation is summarized in Fig. 10 that shows that the performance of variable pitch configuration is superior for low and moderate wind velocities. Performance of both turbine types becomes similar at wind velocities of about 20 km/h.



According to tested configurations observations, the cut-in wind velocity is greater than 17 km/h for the fixed pitch configuration, while the cut-in wind velocity for the variable pitch configuration is at most equal to 12 km/h.

It is obvious that strong winds produce more energy than low and moderate velocity winds. The question is whether strong winds occur with sufficient frequency to make up for poor performance of fixed pitch configuration at low wind velocities. To answer this question, the curve fit equations shown in Fig. 10 have been used to estimate the hypothetical annual energy production using average daily wind velocities recently measured over a one year-long time interval in Oviedo Spain, see Anonymous, 2021. The estimate has been based on the observation that the variable pitch configuration is able to start producing energy when wind velocity reaches 12 km/h, while the fixed pitch configuration cuts-in at 17 km/h (not taking advantage on low and moderate speed winds, but generating more energy for wind velocities greater than 20 km/h). The relationship between produced energy and wind velocity is shown in Fig. 10, for both configurations. Comparison between energy production ability for these two configurations connected to an external electrical resistance of 10 Ohm and for this set of wind data is shown in Table 3.

Table 3 Comparison of energy production estimates for both configurations, during 2020	
Fixed pitch	Variable pitch
0.21 (kWh)	0.67 (kWh)

The variable pitch configuration is clearly superior, even though the accuracy of presented results is not high. E.g., the curve fit approximating the relationship between produced power and wind velocity is based on just two points, for the fixed pitch case. This is, however, caused by the fact that energy production for the fixed pitch configuration occurred only for wind velocities above 17 kmh.

Other interesting observation, based on rotor rundown analysis, is that the braking moment due to aerodynamic resistance constitutes about 40% of the total parasitic moment needed just to turn

the turbine - for both configurations. Drag created by moving turbine parts can be substantially reduced through design modifications. For example, the number of rotating rods per blade could be reduced from three to two (a single blade arm instead of two) and the improvement of their aerodynamic characteristics, for example placing the control rod directly behind the blade arm and shielding both with a fairing that has a cross-section of an airfoil.

Conclusions

Obtained results indicate that the variable blade pitch configuration of a VAWT offers far superior performance for low and moderate wind velocities and for low load resistance values. Those are precisely the typical conditions for urban and residential environments and applications of growing interest, such as car or renewable energy production system batteries.

Please note that, although the presented results have been obtained in relatively primitive conditions, obtained information shows **differences** between two systems tested in the same environment.

Aerodynamics of the variable configuration can be improved by substituting the tested system – with two arms and one control rod per blade – with a system that has just a single arm with a cross-section of an airfoil per blade and a control rod built into the arm. See Fig. 11, where the fairings of arm/blade unions and of the hub are not sketched. The eccentric control link used to control blade pitch in the tested variable pitch configuration has been replaced with a cam and follower mechanism, which is a much more compact and robust system.

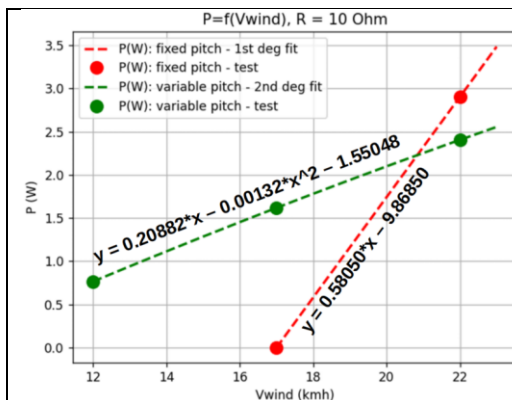


Fig. 10 Mechanical power generated vs wind velocity

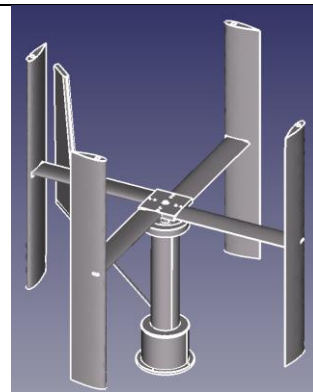


Fig. 11 Variable pitch VAWT with more efficient aerodynamics. The cam and follower mechanism built into the hub, not shown.

References

- Anonymous 2020, "FY42EM150A Product Description," <https://sz.xfoyo.com/a/bujindianji/liangxiangbujindianji/138.html>
- Anonymous, 2021, "Climate Oviedo," <https://en.tutiempo.net/climate/2020/ws-80150.html>
- Benedict, M. and Chopra I., 2016, "Aerodynamics of a Small-Scale Vertical-Axis Wind Turbine with Dynamic Blade Pitching," AIAA Journal, Vol. 54, No. 3, March.
- Erickson D. W., Wallace J. J. and Peraire J., 2011, " Performance Characterization of Cyclic Blade Pitch Variation on a Vertical Axis Wind Turbine," AIAA Paper 2011-638, Proceedings of 49th AIAA Aerospace Sciences Meeting including the New Horizons Forum and Aerospace Exposition, 04 January 2011 - 07 January.
- Miao, Y., 2019, "Advanced Electric Vehicle Fast-Charging Technologies," Energies, Vol. 12, p. 1839, https://www.researchgate.net/figure/Battery-internal-resistance-is-a-function-of-battery-temperature-The-internal-resistance_fig4_333115032

Appendix

Fabrication and calibration

All the plastic parts used in this project, including rotor blades, have been 3d printed using an excellent Prusa Research printer, see Figs. A1 and A2.



Fig. A1 Half of the 400 mm-long blade during printing, using Prusa PETG filament.

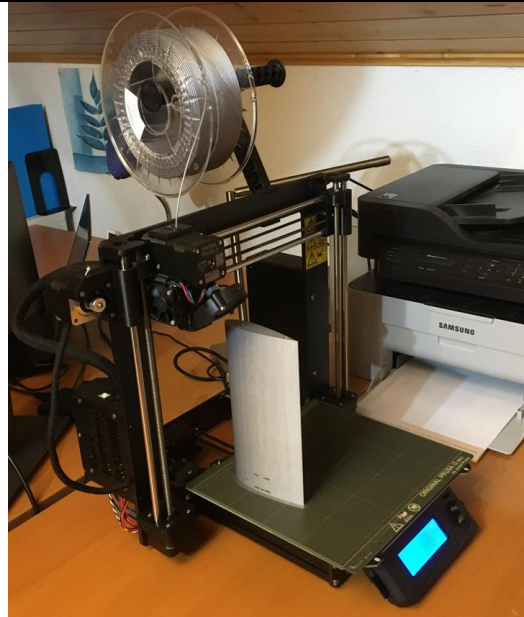


Fig. A2 A finished half-blade component.

Another very useful tool was a numerically controlled hot-wire Styrofoam cutter built using documentation available on the Internet. See, Fig. A3 where 1 is the hot wire, 2-a cut Styrofoam plate, 3-guides to control the plate travel during the cutting process and, 4-a tray with control and power electronics, connected with the computer visible in the background. The control system is

based on Arduino Uno microprocessor with open-source numerical control software GRBL. That tool has been used to cut the contraction nozzle seen in Fig. 3. It has been used, as well, to scan the distribution of velocities in the airflow conditioned by the contraction nozzle.



Fig. A3 The styrofoam cutter system.

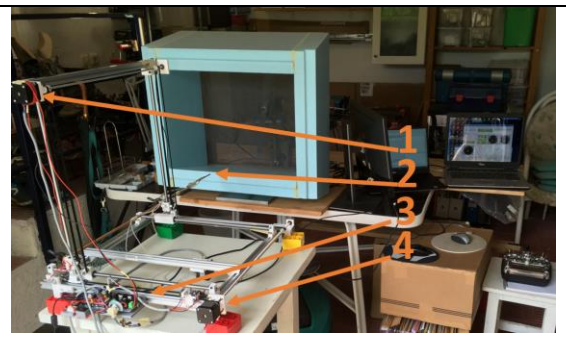


Fig. A4 The flow velocity distribution scanner.

The system used to measure airflow velocity distribution in order to improve the accuracy of obtained results and to validate the rotor aerodynamics model being developed in parallel, is shown in Fig. A4, where 1 is a stepper motor to translate the Pitot tube vertically, 2 – the Pitot tube, 3 – the tray with control and power electronics and, 4-the stepper motor to translate the Pitot tube horizontally.

The test stand for calibration of the load cell used to measure the mechanical power generated at VAWT shaft is shown in Fig. A5, where 1 is Arduino Uno, 2 – the load cell with resolution of 1 G, 3 – the generator casing/support and, 4-the portion of turbine body added to make measurements of the generated shaft power possible, but not necessary for energy generation. The “inner workings” of the turbine are shown in Fig. A6.

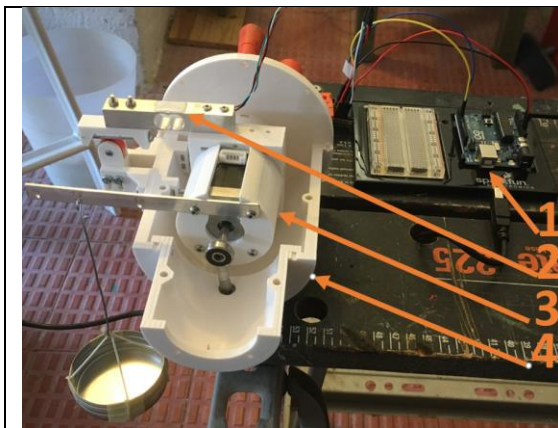


Fig. A5 The test stand for load cell calibration.

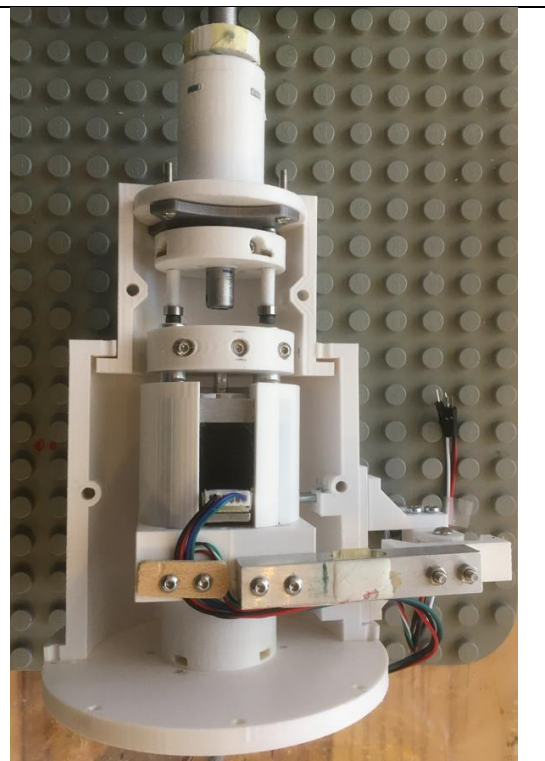
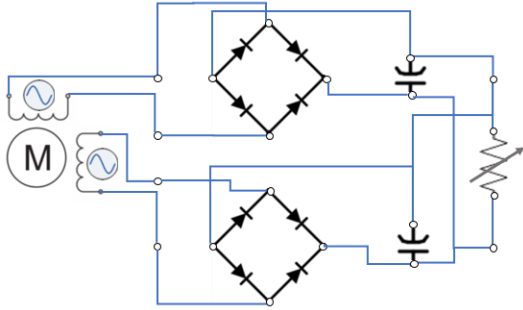
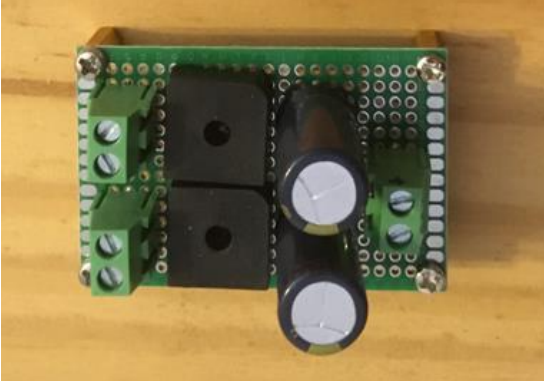
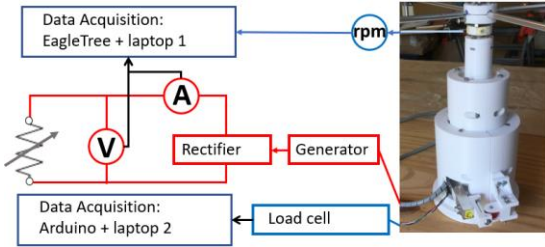



Fig. A6 Details of turbine interior.

Figs. A7 and A8 show the schematic and its physical implementation, respectively, of the custom-made two-phase AC/DC rectifier.

	
<p>Fig. A7. Two-phase rectifier schematic, connected in parallel.</p>	<p>Fig. A8. Custom fabricated two-phase rectifier, with two bridge rectifiers Vishay KBPC104, 35 V and capacitors 1000µF, 35 V – connected in parallel.</p>

Figs. A9 shows a schematic of the test apparatus used to measure tested VAWT's power output. Fig. A10 presents a transmission considered for the tested turbine to get closer to the nominal angular velocity of the generator. However, the increase in moment needed to turn the turbine, needed to maintain constant power at lower revolutions, proved to hike the cut-in velocity too much, and the idea was abandoned.

	
<p>Fig. A9. The test apparatus</p>	<p>Fig. A10. Integration of the timing belt-based transmission with the VAWT body.</p>